



OPEN

Internal dose assessment of ^{148}Gd using isotope ratios of gamma-emitting ^{146}Gd or ^{153}Gd in accidentally released spallation target particles

C. Rääf¹✉, V. Barkauskas², K. Eriksson Stenström², C. Bernhardsson¹ & H. B. L. Pettersson^{3,4}

The pure alpha emitter ^{148}Gd may have a significant radiological impact in terms of internal dose to exposed humans in case of accidental releases from a spallation source using a tungsten target, such as the one to be used in the European Spallation Source (ESS). In this work we aim to present an approach to indirectly estimate the whole-body burden of ^{148}Gd and the associated committed effective dose in exposed humans, by means of high-resolution gamma spectrometry of the gamma-emitting radiogadolinium isotopes ^{146}Gd and ^{153}Gd that are accompanied by ^{148}Gd generated from the operation of the tungsten target. Theoretical minimum detectable whole-body activity (MDA) and associated internal doses from ^{148}Gd are calculated using a combination of existing biokinetic models and recent computer simulation studies on the generated isotope ratios of $^{146}\text{Gd}/^{148}\text{Gd}$ and $^{153}\text{Gd}/^{148}\text{Gd}$ in the ESS target. Of the two gamma-emitting gadolinium isotopes, ^{146}Gd is initially the most sensitive indicator of the presence of ^{148}Gd if whole-body counting is performed within a month after the release, using the twin photo peaks of ^{146}Gd centered at 115.4 keV (MDA < 1 Bq for ingested ^{148}Gd , and < 25 Bq for inhaled ^{148}Gd). The corresponding minimum detectable committed effective doses will be less than 1 μSv for ingested ^{148}Gd , but substantially higher for inhaled ^{148}Gd (up to 0.3 mSv), depending on operation time of the target prior to the release. However, a few months after an atmospheric release, ^{153}Gd becomes a much more sensitive indicator of body burdens of ^{148}Gd , with a minimum detectable committed effective doses ranging from 18 to 77 μSv for chronic ingestion and between 0.65 to 2.7 mSv for acute inhalation in connection to the release. The main issue with this indirect method for ^{148}Gd internal dose estimation, is whether the primary photon peaks from ^{146}Gd and ^{153}Gd can be detected undisturbed. Preliminary simulations show that nuclides such as ^{182}Ta may potentially create perturbations that could impair this evaluation method, and which impact needs to be further studied in future safety assessments of accidental target releases.

The European Spallation Source (ESS), located north-east of the city of Lund in south-western Sweden, is designed to be the most powerful neutron source in the world using a 5 MW proton beam irradiation against a tungsten target^{1–3}. An inevitable side effect of neutron generation during spallation reactions is the production of various radionuclides in the spallation source. During a 5 years operation of the ESS tungsten target, it is estimated that a number of gamma emitters will be produced, e.g. ^{187}W (> 10^{16} Bq) and ^{172}Hf (> 10^{15} Bq), as well the pure beta emitters such as ^3H (~ 10^{15} Bq) and pure alpha emitters as ^{148}Gd (> 10^{14} Bq)². The national competent authority in Sweden regarding emergency preparedness (Swedish Radiation Safety Authority, SSM) commissioned ESS to elaborate potential technical scenarios that could lead to an atmospheric release of spallation source particles³. Of these scenarios SSM considered the one involving loss of cooling of the spallation source while the neutron production operates at full effect (5 MW), being the one that dimensions the local emergency planning zone. Within minutes of proton beam irradiation of the tungsten target, the temperature increase in

¹Medical Radiation Physics, Department of Translational Medicine, Malmö, Lund University, 205 02 Malmö, Sweden. ²Division of Nuclear Physics, Department of Physics, Lund University, 221 00 Lund, Sweden. ³Department of Radiation Physics, IMV, Faculty of Health Sciences, Linköping University, 581 85 Linköping, Sweden. ⁴These authors contributed equally: H. B. L. Pettersson. ✉email: christopher.raaf@med.lu.se

Nuclide	$T_{1/2}$ (d)	Decay mode	Predominant α - or γ -lines (keV; emission probability, n_g)
^{146}Gd	48.3	Electron capture, gamma to ^{146}Eu ($T_{1/2} = 4.61$ days with principal gamma lines at 633.1 and 634.1 keV; sum of $n_g = 0.809$)	154.6 (0.47) 114.7 (0.441) 115.5 (0.441)
^{153}Gd	240.4	Electron capture, gamma to ^{153}Eu (stable)	97.4 (0.29) 103.2 (0.211)
^{148}Gd	76.4	Alpha emission to ^{144}Sm (stable)	3271.21 (1)

Table 1. Alpha and photon energies (keV) and associated emission probability, n_g , of the emission lines of gadolinium isotopes generated from proton irradiation of a W target⁹.

the target will in this event cause a fraction of the tungsten to melt and oxidize. About 20 kg of this fraction, including evaporated contaminated moderator water, will then be released through the pressure relief system to the surrounding atmosphere at a stack height of 30 m altitude. An additional release of tungsten (<0.2 kg) will occur more than 80 min later in this process when hydrogen deflagration will eject about 0.5% of the remaining melted and oxidized target material into the atmosphere. In this accident scenario, target particles containing radionuclides, such as ^{172}Hf , ^{182}Ta , and ^{187}W , have been estimated to be of largest radiological importance in terms of external exposure of humans from ground deposition of release radionuclides^{3–6}. However, in terms of internal exposure by inhalation or ingestion through contaminated foodstuff, the single most important radionuclide in estimated release scenarios is the pure alpha emitter ^{148}Gd ($E_\alpha = 3.2$ MeV, $T_{1/2} = 74.6$ y)³, due to its high dose coefficient of up to 3×10^{-5} Sv Bq⁻¹, which is comparable to alpha emitters such as ^{223}Ra and ^{238}Pu ⁷.

Rääf et al.⁸ estimated the minimum detectable intakes of the gamma emitting spallation source nuclides ^{172}Hf , ^{182}Ta , and ^{187}W to be 0.26, 0.04, and 65 kBq, respectively, when measured 24 h post intake using a large (123% relative efficiency), high-resolution HPGe in vivo whole-body counter in a low-background environment. When considering the alpha emitting ^{148}Gd this technique is not directly available for internal dose assessments. However, since production of ^{148}Gd in the tungsten target is accompanied by other gadolinium isotopes that are gamma emitters, it has been suggested that the presence of ^{148}Gd could be indirectly estimated by in gamma spectrometry provided that the isotope ratios of the gamma-emitting isotopes are known³. Potential isotopes for such assessment are ^{146}Gd ($T_{1/2} = 48.3$ days) and ^{153}Gd ($T_{1/2} = 240.4$ days). The three principal gadolinium isotopes generated in a tungsten target from proton irradiation are listed in Table 1 together with their respective physical half-time and decay mode⁹.

The aim of this study is to suggest a method of indirect whole-body gamma ray counting of ^{148}Gd that could facilitate a rapid assessment of the internal doses to affected humans after dispersion of ^{148}Gd to the environment. By combining theoretical isotope ratios of $^{146}\text{Gd}/^{148}\text{Gd}$ and $^{153}\text{Gd}/^{148}\text{Gd}$ in an irradiated W target of the ESS, based on simulations presented in a previous study by Barkauskas and Stenström², with biokinetic relationships derived from models presented by the International Commission of Radiological Protection (ICRP), we aim to estimate the minimum detectable whole-body burdens and associated internal dose from the alpha emitter ^{148}Gd for a high efficiency high-resolution whole-body counting set-up presented in detail by Rääf et al.⁸. No detailed modelling of the fate of gadolinium in the terrestrial environment outside of ESS has been published, although internal estimates exist, which use e.g. americium and lanthanum as a chemical analogues when applying values for transfer parameters used in terrestrial models defined by IAEA (2001)¹⁰. Current studies on the ecological behaviour of gadolinium in this environment is launched (Lund University, 2019¹¹). In absence of explicit estimates on the ecological half-time of gadolinium in vital environmental compartments such as crops, pasture, garden products and fresh water, we have conservatively assumed the following: i) inhalation of airborne gadolinium occurs momentarily after the accident, ii) during the first year upon release, there will be a transfer of radioactive gadolinium via the food chain to man, resulting in a constant daily ingestion rate.

Theoretical outline and methods

Biokinetic model. ICRP has presented a systemic biokinetic model for gadolinium¹⁰. Like all rare earth metals, gadolinium has a low uptake into tissue when ingested. ICRP 141¹² presents a systemic biokinetic model for Gd and proposes a very low gastrointestinal (GI) uptake fraction (f_1) of 0.0005 based on literature surveys¹³. The internal doses incurred are hence estimated to be rather low in relation to the activity intake, compared with more easily incorporated radionuclides such as radiocaesium, which is associated with fission products released from nuclear accidents or nuclear weapons debris. However, given the average transit time of 36 h for foodstuffs through the GI tract (described by, e.g., ICRP 100¹⁴), intakes of gadolinium by humans must still be considered, as the gadolinium isotopes may cause internal exposure during its passage time as well. In case of accidental releases from the tungsten target, the likely physiochemical form would be as particles, volatilized tungsten, and tungsten oxides^{15,16}. When using that model, there appears to be a long time (<1 y) before reaching the equilibrium whole-body stable gadolinium level at chronic intake. An ingestion of 1 Bq day⁻¹ of any of the listed gadolinium isotopes listed in Table 1 corresponds to an infusion of 0.0005 Bq/day to systemic tissues. At 1 year after onset of the chronic intake of 1 Bq day⁻¹ of a given gadolinium isotope, the systemic gadolinium content in a human will be 0.125 Bq, 0.025 Bq, and 0.075 Bq for ^{148}Gd , ^{146}Gd , and ^{153}Gd , respectively. Moreover, it is estimated that equilibrium in the whole-body content of stable gadolinium is not reached until after 30 years of constant intake. For ^{148}Gd , the equilibrium level is then estimated to be approximately 0.9 Bq per 1 Bq daily ingestion.

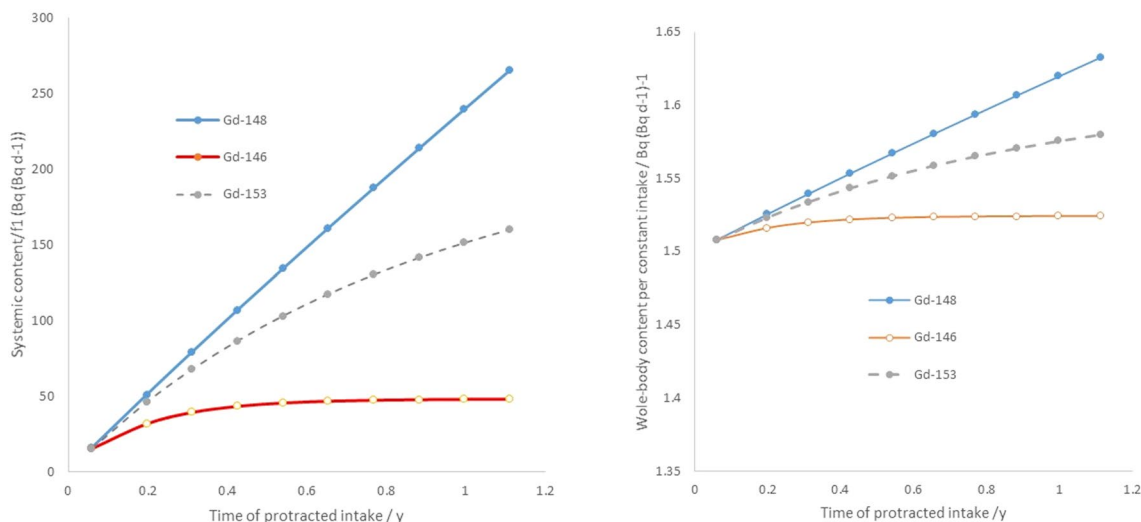


Figure 1. Left: Build-up of systemic ¹⁴⁶Gd, ¹⁴⁸Gd and ¹⁵³Gd in human tissue after a daily intake of 1 Bq day⁻¹ per isotope, normalised to uptake fraction *f*₁(=0.0005). Right: Build-up of whole-body activity (sum of systemic and GI contents) for ^{146,148,153}Gd normalized per daily intake of each isotope, *q*_{146,148,153}(*t*).

For systemically incorporated Gd, a large fraction will be found in soft tissue (approximately 17.3%). However, a yet larger fraction (55.1%) will be found in the cortical bone surface. This will result in a nearly homogeneous distribution in the whole body. However, due to the extremely low GI uptake (*f*₁ = 0.0005 according to ICRP 141¹²), it is not anticipated that the component of systemic uptake of gadolinium will be important in comparison to the fraction of gadolinium in the GI tract. Hence, for in vivo whole-body counting of gamma emitting gadolinium isotopes in subjects who have chronically ingested radiogadolinium, a measurement geometry assuming major uptake in the abdominal region is more appropriate (See section “Estimating ¹⁴⁸Gd whole-body burden and cumulative committed effective dose by means of high-resolution gamma spectrometry”).

Relating ¹⁴⁸Gd body burden with activity ratios of released gamma emitting gadolinium isotopes. Some model derivations are needed to yield expressions that relate what is measurable by means of whole-body counting in a scenario with widespread release of radioactive gadolinium with a certain distribution between released gadolinium isotopes, ¹⁴⁶Gd, ¹⁴⁸Gd and ¹⁵³Gd, to incurred committed effective dose of exposed subjects from ¹⁴⁸Gd. Considering a passage time (residence time) in the GI tract of 36 h¹⁴, a chronic ingestion of 1 Bq/day of a given gadolinium isotope will lead to an equilibrium level of 1.5 Bq per Bq/day intake in the GI tract, if disregarding the low fraction (*f*₁ = 0.0005) that has been taken up systemically. Given the long physical half-life of ¹⁴⁸Gd (*T*_{1/2} = 76.4 y), this means that, after 1 year of chronic constant intake of ¹⁴⁸Gd, the expected gadolinium abundance in the GI content during passage will be more than one order of magnitude larger than the fraction of ¹⁴⁸Gd being incorporated systemically. Thus, in practice for protracted internal exposures, radioactive gadolinium will predominantly be found in the abdominal part of the body (Fig. 1, Right). It will also mean that, even for very long protracted intakes, the systemic gadolinium will only be a small fraction of the whole-body burden at any given time after the onset of the intake.

For short-lived gadolinium isotopes, the colon doses are more relevant over the long term compared with the dose to systemic tissue. The whole-body activity of a given gadolinium isotope, *Q*_{Gd}, at any given time is the sum of the component in the GI contents, *Q*_{Gd,GIcont}(*t*), and the systemically incorporated Gd, *Q*_{Gd,sys}(*t*):

$$Q_{Gd}(t) = Q_{d,GIcont}G(t) + Q_{Gd,sys}(t) \tag{1}$$

Using¹⁴ for the systemic component and a 36 h retention time of the inert fraction of gadolinium in the GI tract, the gadolinium content as a function of time after a constant protracted daily intake, *I*_{Gd} (Bq day⁻¹), can be expressed in terms of intake normalized body content, *q*_{Gd}(*t*):

$$q_{Gd}(t) = \frac{Q_{Gd}(t)}{I_{Gd}} = \left(\frac{Q_{Gd,GIcont}(t) + Q_{Gd,sys}(t)}{I_{Gd}} \right) = Q_{Gd,GIcont}(t) \cdot h_{Gd}(t) + Q_{Gd,sys}(t) \cdot m_{Gd}(t) \tag{2}$$

contents and systemic tissue, respectively, normalized against the daily protracted intake *I*_{Gd}. For ¹⁴⁸Gd, the normalized body content *q*_{Gd-148}(*t*) as a function of time, *t* (d), after start of chronic ingestion of 1 Bq day⁻¹, can be expressed as follows:

$$q_{Gd-148}(t) = 1 \cdot t; \quad \text{if } t < 1.5 \text{ d} \\ 1.5 + 0.93 \cdot \left(1 + e^{-\frac{\ln 2}{1821} \cdot t} \right); \quad \text{if } t \geq 1.5 \text{ d} \tag{3}$$

Equation 3 is obtained by curve regression from the combination of the systemic biokinetic model in¹² and the ICRP colon model described in¹⁴. In the right from of Fig. 1 the plot of Eq. (3) is given for ¹⁴⁶Gd, ¹⁴⁸Gd and ¹⁵³Gd, respectively.

The whole-body activity of the gamma-emitting gadolinium isotopes ¹⁴⁶Gd and ¹⁵³Gd at a given time *t* after the onset of the chronic intake of ¹⁴⁸Gd, I_{Gd-148} , can be related to the whole-body activity of the alpha emitter ¹⁴⁸Gd with the corresponding retention of the accompanied gamma-emitting gadolinium isotopes ¹⁴⁶Gd and ¹⁵³Gd. Thus, for a scenario of intakes from a release containing a composition of different radio-gadolinium isotopes, the whole-body activity of ¹⁴⁸Gd, Q_{Gd-148} , can be expressed in terms of the corresponding whole-body activity of either of the gamma-emitting radionuclides ¹⁴⁶Gd or ¹⁵³Gd, using the following relationships:

$$Q_{Gd-148}(t) = Q_{Gd-146,GIcont}(t) \cdot h_{148/146}(t) + Q_{Gd-146,syst}(t) \cdot m_{148/146}(t) = k_{148/146}(t) \cdot Q_{Gd-146}(t) \quad (4)$$

or

$$Q_{Gd-148}(t) = Q_{Gd-153,GIcont}(t) \cdot h_{148/153}(t) + Q_{Gd-153,syst}(t) \cdot m_{148/153}(t) = k_{148/153}(t) \cdot Q_{Gd-153}(t) \quad (5)$$

where $h_{148/146}(t)$ is the time-dependent activity ratio between ¹⁴⁶Gd and ¹⁴⁸Gd in the GI contents divided by the daily intake of ¹⁴⁸Gd, I_{Gd-148} (Bq day⁻¹), and $h_{153/146}(t)$ is the corresponding activity ratio for ¹⁵³Gd and ¹⁴⁸Gd. Moreover, in analogy with the expression in Eq. (2), the term $m_{148/146}(t)$ in Eq. (4) is the activity ratio at time *t* between ¹⁴⁶Gd and ¹⁴⁸Gd, divided by I_{Gd-148} in the systemic tissues, and $m_{153/146}(t)$ is the corresponding ratio for ¹⁵³Gd and ¹⁴⁸Gd. In turn, the expressions in Eqs. (3) and (4) can be rewritten as a time-dependent relationship between the whole-body burden of Q_{Gd-148} and Q_{Gd-146} and Q_{Gd-153} , respectively, in terms of the time-dependent scaling factors $k_{148/146}$ and $k_{148/153}$, respectively. The purpose of the expressions in Eqs. (3) and (4) is thus to relate the whole-body burden of the alpha-emitting ¹⁴⁸Gd with quantities Q_{Gd-148} and Q_{Gd-153} , which are measurable by means of whole-body counting.

Since for a chronic ingestion of radiogadolinium $Q_{Gi-cont} > Q_{syst}$, Eqs. (3) and (4) can virtually be rewritten as

$$Q_{Gd-148}(t) = Q_{Gd-146,GIcont}(t) \cdot h_{148/146}(t) \sim k_{148/146}(t) \cdot Q_{Gd-146}(t) \quad (6)$$

or

$$Q_{Gd-148}(t) = Q_{Gd-153,GIcont}(t) \cdot h_{148/153}(t) \sim k_{148/153}(t) \cdot Q_{Gd-153}(t) \quad (7)$$

The factors $k_{148/146}(t)$ and $k_{148/153}(t)$ are in turn given by the initial activity proportions at the start of the intake (i.e., at time *t* = 0). If the initial activity ratio between ¹⁴⁸Gd and ¹⁴⁶Gd is denoted as $a_{146/148}$, and the ratio between ¹⁴⁸Gd and ¹⁵³Gd is denoted as $a_{153/148}$, then the values of $h_{148/146}(t_0)$ and $m_{148/146}(t_0)$ will be equal to $1/a_{146/148}$, and the values of $h_{148/153}(t_0)$ and $m_{148/153}(t_0)$ will be equal to $1/a_{153/148}$. Likewise, the factors $k_{148/146}(t)$ and $k_{148/153}(t)$ will then be equal to $1/a_{146/148}$ and $1/a_{153/148}$, respectively, at *t* = *t*₀. In this study, $a_{146/148}$ and $a_{153/148}$ are simulated using the FLUKA code^{17,18}, where *t*₀ = time of the release to the environment. Assuming equal biochemical and biokinetic behavior for all radiogadolinium isotopes, the daily intake of ¹⁴⁶Gd and ¹⁵³Gd will then be $I_{Gd-148}/a_{146/148}$ and $I_{Gd-148}/a_{153/148}$, respectively. In this computational study, no account of ecological turnover of dispersed gadolinium was considered, meaning that the effective ecological half-times of gadolinium isotopes are assumed to be equal to their corresponding physical half-lives.

Committed effective dose calculations. ICRP⁷ provides data on committed effective dose coefficients per unit intake of gadolinium isotopes. The committed effective dose, E_{Gd-148} (mSv), incurred at time *t* (d) after the start of a chronic intake of ¹⁴⁸Gd, denoted as I_{Gd-148} (Bq day⁻¹), can then be expressed as:

$$E_{Gd-148}(t) = I_{Gd-148} \cdot t \cdot e_{Gd-148} \quad (8)$$

where e_{Gd-148} (mSv Bq⁻¹) is the committed effective dose coefficient taken from ICRP 119⁷ for an adult person. The coefficient refers to the time-integrated effective dose incurred upon intake (ingestion or inhalation) of a radionuclide. For the alpha emitter, this coefficient is $5.5 \cdot 10^{-5}$ mSv Bq⁻¹ for ingestion of ¹⁴⁸Gd, which is more than 50 times higher than for ingestion of ¹⁴⁶Gd and 200 times higher than for ingestion of ¹⁵³Gd. The corresponding formulae for ¹⁴⁶Gd and ¹⁵³Gd are

$$E_{Gd-146} = I_{Gd-146} \cdot t \cdot e_{Gd-146} = I_{Gd-148} \cdot a_{146/148}(t) \cdot t \cdot e_{Gd-146} = I_{Gd-153} \cdot a_{146/153}(t) \cdot t \cdot e_{Gd-146} \quad (9)$$

Exploiting that I_{Gd-148} is equal to the ratio $Q_{Gd-148}(t)/q_{Gd-148}(t)$, Eq. (8) can be expressed as

$$E_{Gd-148}(t) = (Q_{Gd-148}(t)/q_{Gd-148}(t)) \cdot t \cdot e_{Gd-148} \quad (10)$$

Q_{Gd-148} in turn can be expressed through either Eqs. (3) or (4) by relating it to the corresponding whole-body activities of ¹⁴⁶Gd and ¹⁵³Gd, respectively. The cumulative committed effective dose as a function of time per a chronic daily intake of I_{Gd-148} (Bq day⁻¹) can then be deduced by the following:

$$E_{Gd-148}(t) = e_{Gd-148} \cdot (k_{148/146}(t) \cdot Q_{Gd-146}(t))/q_{Gd-148}(t) \cdot t \quad (11)$$

or

$$E_{Gd-148}(t) = e_{Gd-148} \cdot (k_{148/153}(t) \cdot Q_{Gd-153}(t))/q_{Gd-148}(t) \cdot t \quad (12)$$

Hence, by numerically computing the time-dependent ratios q_{Gd-148} , $k_{148/146}(t)$, and $k_{148/153}(t)$ using the ICRP models ICRP 100¹⁴, ICRP 119⁷, and ICRP 141¹², the whole-body activity and associated cumulative committed effective dose from the alpha emitter ^{148}Gd can be related to the measurable quantities Q_{Gd-146} or Q_{Gd-153} for a given set of isotope release ratios, $a_{148/146}$ and $a_{148/153}$, respectively.

Inhalation of radiogadolinium. Acute intakes through inhalation can lead to significant proportions of systemic activities of ^{148}Gd , even after full excretion of the initial GI contents. It is assumed that inhalation of radiogadolinium is only relevant during the immediate phase after a release event. A varying amount of the inhaled ^{148}Gd will then be taken up into the systemic tissues depending on the absorption rate from respiratory tract to blood (ICRP¹²). If inhaled in oxide form, most of the gadolinium will be confined to the lungs, even months after inhalation. However, when considering the total body burden of ^{148}Gd , Q_{Gd-148} (Bq), for an acute inhalation of ^{148}Gd , $I_{inh,Gd-148}$ (Bq), the measured body burdens of ^{146}Gd or ^{153}Gd at time t after intake can then be expressed as

$$Q_{Gd-146}(t) = I_{inh,Gd-148} \cdot a_{146/148}(t=0) \cdot R(t); Q_{Gd-153}(t) = I_{inh} \cdot a_{153/148}(t=0) \cdot R(t) \quad (13)$$

where $R(t)$ is the retention curve for ^{146}Gd (N.B. not decay corrected) upon inhalation of the radiogadolinium. To our knowledge, it is not well-known which particle diameter should be expected in different accident scenarios¹³. Given the lack of this knowledge, here we use the retention derived from the ICRP model¹², with inhalation parameters s_b ($=0.021 \text{ day}^{-1}$), s_r ($=0.3 \text{ day}^{-1}$), s_s ($=0.002 \text{ day}^{-1}$), f_r ($=0.5$), and f_b ($=0.07$), which are essentially based on a human volunteer study on inhalation of $^{153}\text{Gd}_2\text{O}_3$ particles in 2002¹⁹. The parameters correspond to a moderate rate of absorption (Type M) and to an activity median aerodynamic diameter (AMAD) particle size of $2.2 \mu\text{m}$ (ICRP¹²).

Particle size is an important parameter affecting the dose calculations. The Swedish Radiation Safety Authority uses an AMAD of $1 \mu\text{m}$ in their dispersion and dose calculations for the boundary accident scenario (smaller particle sizes are not applicable in the dispersion model used by SSM) and has performed a sensitivity analysis for particles with an AMAD $> 5 \mu\text{m}^3$. According to the bioassay software tool, IMBA (Integrated Modules for Bioassay Analysis²⁰), the particle size assumed here will yield a committed effective dose of $1.26 \cdot 10^{-5} \text{ Sv}$ per unit inhaled Bq ^{148}Gd , which is about a factor of two less than that for a Class F (fast absorption rate) particle in the size range 1 to $5 \mu\text{m}$ but somewhat higher than the corresponding values for M Class particles in the same size range. The corresponding effective doses for ^{146}Gd and ^{153}Gd are orders of magnitude lower: 7.6 and 2.5 nSv Bq^{-1} , respectively.

Hence, $I_{inh,Gd-148}$ can be deduced from $a_{146/148}$, the $R(t)$ function, and the measured whole-body burden of the gamma-emitting ^{146}Gd or ^{153}Gd . The corresponding committed effective dose from ^{148}Gd will then be

$$\begin{aligned} E_{Gd-148} &= I_{inh,Gd-148} \cdot e_{Gd-148,inh} = (Q_{Gd-146}/a_{146/148}(t=0) \cdot R(t)) \cdot e_{Gd-148,inh} \\ &= (Q_{Gd-146}/a_{153/148}(t=0) \cdot R(t)) \cdot e_{Gd-148,inh} \end{aligned} \quad (14)$$

where $e_{Gd-148,inh}$ is the dose coefficient computed by the software IMBA, given the retention functions and associated parameters mentioned previously. Thus, the committed effective dose, E_{Gd-148} , from an acute inhalation of ^{148}Gd could be estimated through a whole-body burden measurement of ^{146}Gd or ^{153}Gd .

Target and release activity ratios of ^{146}Gd , ^{148}Gd , and ^{153}Gd . Activity ratios $a_{146/148}$ and $a_{153/148}$ were evaluated using data obtained from simplified ESS target modeling of the radionuclide composition [2new]. All major components of the ESS target were included in the model with simplified geometries. The FLUKA code was used for calculations, as it is suitable for calculations of particle transport and interactions with matter using the Monte Carlo method^{17,18}. We obtained about a factor of 2 higher absolute values of ^{148}Gd in comparison with other authors^{21,22}, and these differences can be attributed to differences in spallation and nuclide evaporation models. Unfortunately, there are no experimental data yet to evaluate which of the predictions is more accurate regarding absolute values. Activity ratios $a_{146/148}$ and $a_{153/148}$ were calculated for different operation times and decay periods, up to 350 days after 5 years of target operation (designed lifetime of the target).

Estimating ^{148}Gd whole-body burden and cumulative committed effective dose by means of high-resolution gamma spectrometry. In combination with estimated activity ratios of ^{146}Gd , ^{148}Gd , and ^{153}Gd in the spallation target and the biokinetic models described in Eqs. (7) and (13), the minimum detectable activity (MDA) of the alpha emitter ^{148}Gd for a high-resolution whole-body counting system, consisting of a 123% high purity germanium (HPGe) described by Rääf et al.⁸, was calculated. The whole-body counter is calibrated for a uniform body distribution of gamma emitters, but in this study alternative uptake geometries were needed to better mimic the anticipated uptakes of subjects exposed to internal radiogadolinium contamination. Using the VMC in vivo tool (VMC 2018²³), the relative difference in the efficiency calibration of a HPGe whole-body counter between a uniform whole-body distribution of gamma emitters in the energy range 100 to 150 keV, and that of specific organ uptakes could be simulated. In this tool the geometry of lung uptake in male adult phantom was available and used here for acute inhalation of a gamma emitter, whereas an uptake in the liver in the same phantom was used to mimic the calibration factor for a whole-body counting with elevated uptake in the abdominal region. The calibration factors for the 123% HPGe system in the photon energy range of 100 to 150 keV (roughly encompassing the considered gamma lines of ^{146}Gd and ^{153}Gd given in Table 1) could then be corrected by a factor of 2 ($\pm 10\%$ $k=1$) for abdominal region uptake and by a factor of 0.66 ($\pm 10\%$ $k=1$) for lung uptake. The MDA_{Gd-148} value in combination with Eq. (14) could then be used to estimate the corre-

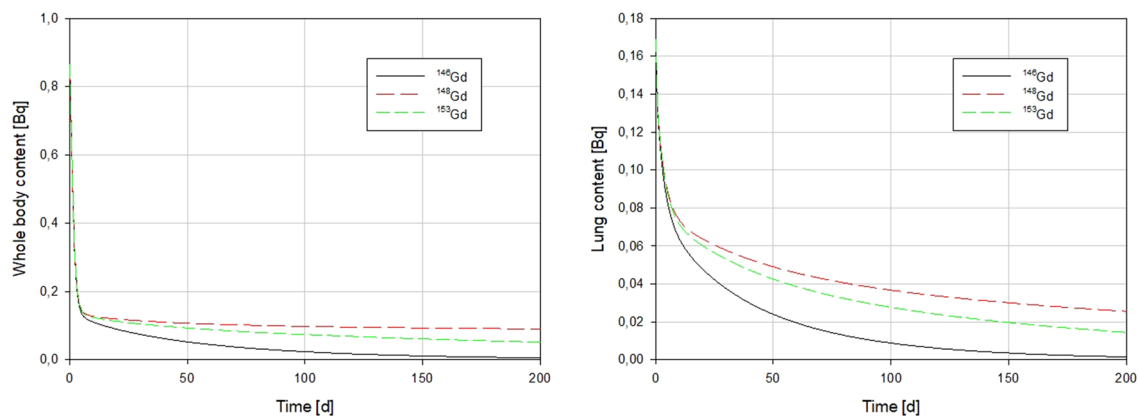


Figure 2. Isotope specific retention curves, $R(t)$, for ^{146}Gd , ^{148}Gd , and ^{153}Gd upon inhalation. Left: Whole body. Right: Lung model taken from ICRP12 using $f_b = 0.07$, $f_r = 0.5$, $s_b = 0.021 \text{ d}^{-1}$, $s_s = 0.002 \text{ d}^{-1}$, and $s_r = 0.3 \text{ d}^{-1}$. Parameters are further explained in ICRP 130²⁴.

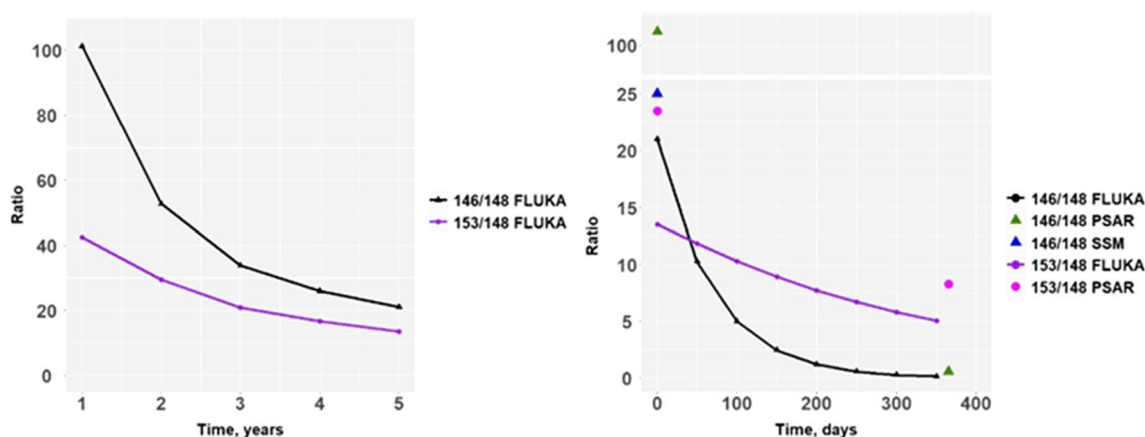


Figure 3. Left: Modeled activity ratios of ^{146}Gd to ^{148}Gd ($a_{146/148}$) and ^{153}Gd to ^{148}Gd ($a_{153/148}$) in the W target as a function of operation time. These values correspond to $a_{146/148}(t_0)$ and $a_{153/148}(t_0)$ in Eqs. 12 and 13. Right: Activity ratios in a W target after 1 y operation as a function of time after the cessation of operation. Values are simulated using FLUKA. Numbers from ESS PSAR (2012)²² and SSM report³ are provided for comparison.

sponding minimum detectable committed effective dose, $MDD_{\text{Gd-148}}$. The MDA and MDD values as a function of time of the after the release, for two different operation times (1 and 5 y) were explored. Finally, the potential perturbations from other gamma lines present will be discussed, based on simulations of gamma spectra.

Results and discussion

Simulated relative W-target inventories of radiogadolinium and assumed daily ingestion after a release. Simulated W-target activity ratios between ^{146}Gd and ^{148}Gd and between ^{153}Gd and ^{148}Gd , respectively, during operation of the ESS target are given in Fig. 2 (left). The corresponding activity ratios for dispersed W-target particles as a function of time after the release are plotted in Fig. 2 (right). The activity ratio values taken from the ESS Preliminary Safety Analysis Report (PSAR)²² and SSM report on emergency preparedness planning around the facility³ are also provided in Fig. 2. The ratios from those reports are higher, i.e., they predict relatively lower activities of ^{148}Gd in comparison with other gadolinium isotopes. Our predictions might be considered more conservative in terms of relative proportion of the alpha emitting gadolinium isotope, but experimental data are necessary to prove this hypothesis. The SSM report³ also suggests that ^{148}Gd deposition on the ground might be monitored using the gamma-emitting ^{146}Gd , considering the activity ratio of these radionuclides.

Note that the abovementioned activity ratios will represent the initial release activity ratios, $a_{146/148}$ and $a_{153/148}$, in the case of an accidental atmospheric release either during or after operation. The resulting daily ingestion of ^{146}Gd and ^{153}Gd normalized to that of ^{148}Gd , assuming only physical decay in the environment, is given in Fig. 3 for a number of different target operation times (1 to 5 y).

Body burdens of ^{148}Gd as a function of time relative to that of ^{146}Gd and ^{153}Gd and its dosimetric effect. Based on the FLUKA simulations of the activity ratios in the target, values of $a_{146/148}$ and $a_{153/148}$ in adult individuals subjected to a protracted intake of environmentally dispersed target material can be estimated.

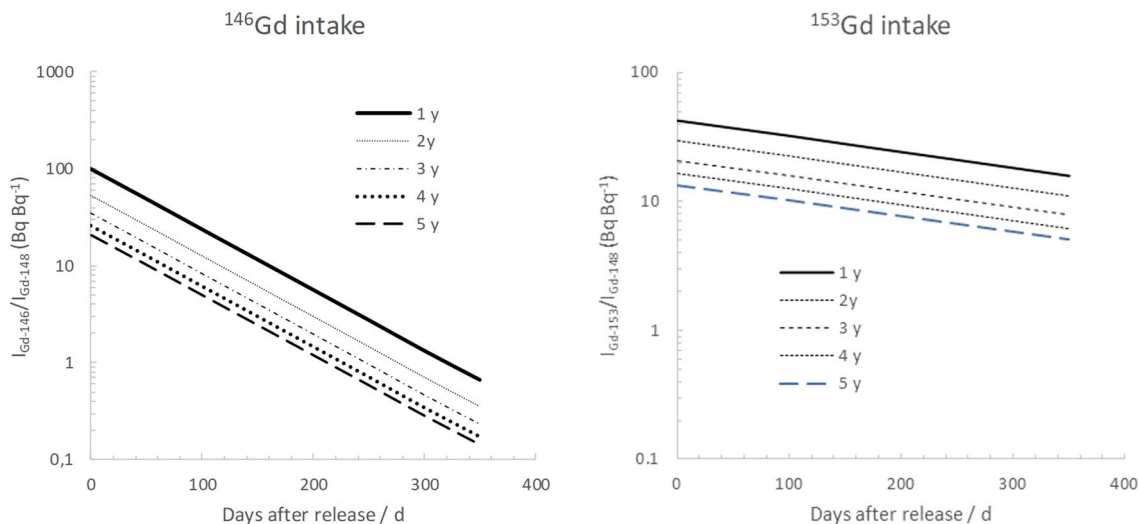


Figure 4. Simulated activity ratios of daily assumed ingestion of ^{146}Gd (left) and ^{153}Gd (right), normalized to that of ^{148}Gd , $I_{\text{Gd-148}}$, as a function of time after an environmental release of particles from the W target. Values are based on simulated activity ratios for different operation times of the ESS tungsten target.

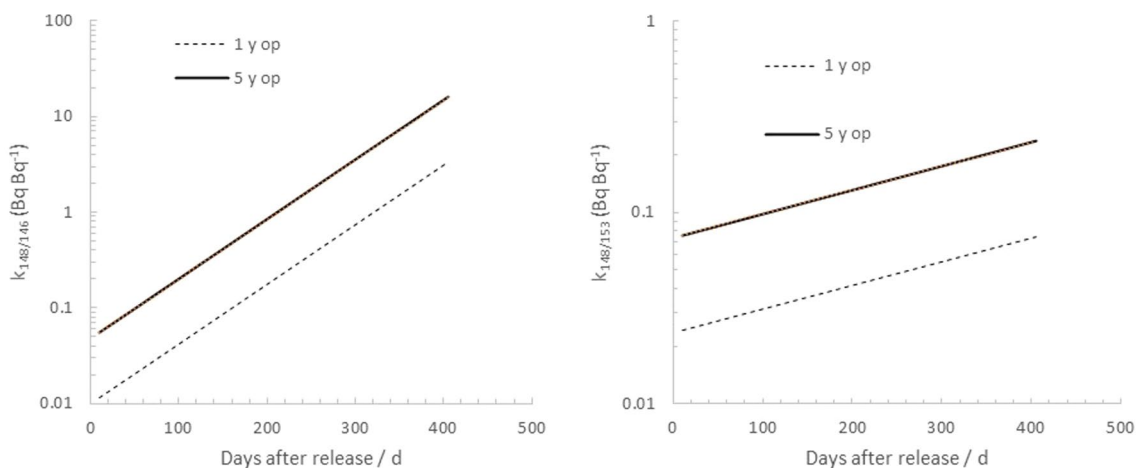


Figure 5. Left: The ratio between whole-body activity of ^{146}Gd and ^{148}Gd as a function of time after onset of chronic intake of 1 Bq d^{-1} of ^{148}Gd after a release from a tungsten target after 1 and 5 y of operation. Right: The same plot for ^{153}Gd .

From these values, the resulting proportions ($k_{148/146}$ and $k_{148/153}$) between the whole-body activity of ^{148}Gd and the gamma emitters ^{146}Gd and ^{153}Gd can be computed for a 1 to 5 years operation time (Fig. 4). It can be seen that, after 1 year of continuous intake of gadolinium isotopes released from a 5 years operation W spallation target, the model predicts a body content of 8.8 Bq of ^{148}Gd for every Bq of ^{146}Gd in an adult person. The corresponding value for ^{153}Gd is much less, only a value of 0.21 (Bq Bq^{-1}). The longer physical half-time of ^{153}Gd will outweigh its lower initial isotopic abundance in the aforementioned release event, and after about 40 days after a release from a 5 years operated W target, the body content of ^{153}Gd will be higher than that of ^{146}Gd .

Figure 5 plots the corresponding cumulative committed effective dose as a function of time per unit whole-body activity of ^{146}Gd and ^{153}Gd , respectively, assuming a daily intake, $I_{\text{Gd-148}}$, of 1 Bq day^{-1} . From these plots, it can be seen that the model predicts a cumulative committed effective dose of $0.30 \mu\text{Sv}$ from ^{148}Gd per detected activity (Bq) of ^{146}Gd in the whole body, if observed 1 years post release of the W target (5 years operation). For ^{153}Gd , this value is considerably lower: 7.1 nSv per unit observed whole-body activity (Bq) of ^{153}Gd . This implies that the detection of ^{153}Gd in vivo will, in theory, be a much more sensitive indicator of ^{148}Gd cumulative committed effective dose than ^{146}Gd when surveying potentially affected persons, already one-month post release from the W target.

The relative contributions to the cumulative committed effective dose from $^{146,153}\text{Gd}$ and ^{148}Gd are given in Fig. 6. Only after some months after the start of the protracted radiogadolinium ingestion does the alpha emitter ^{148}Gd account for the larger part of the cumulative committed effective dose from the three major gadolinium isotopes. One year after the onset of the ingestion, the radionuclide will account for 89% of the cumulative effective dose incurred from the three major gadolinium isotopes for an adult.

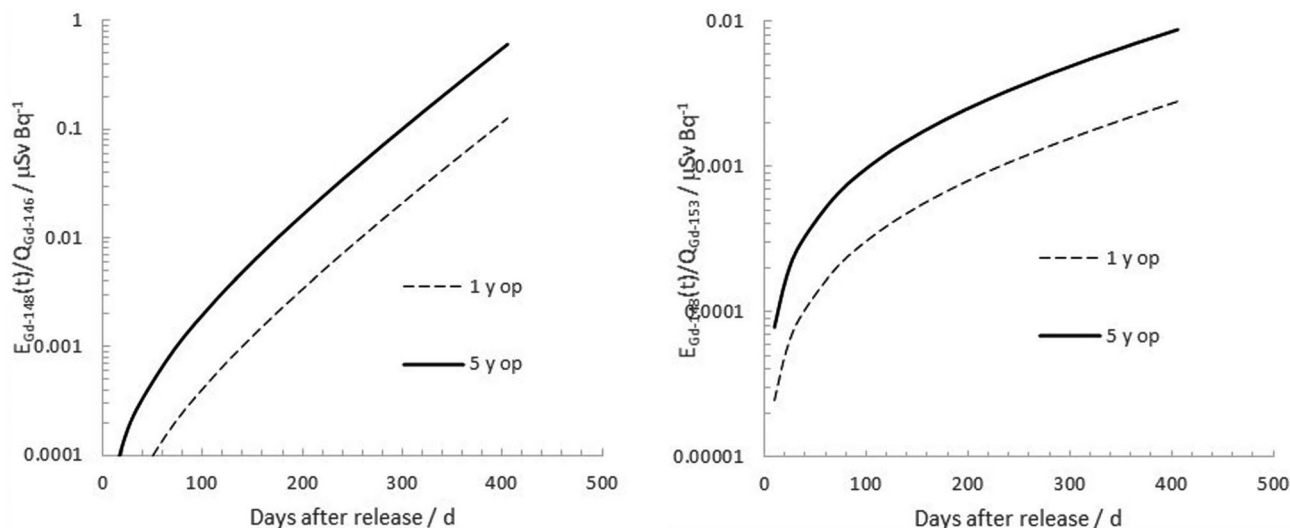


Figure 6. Left: Cumulative committed effective dose from ¹⁴⁸Gd per measured whole-body burden of ¹⁴⁶Gd, $E_{Gd-148}(t)/Q_{Gd-146}$, as a function of time after onset of chronic ingestion of 1 Bq d⁻¹ of ¹⁴⁸Gd. Right: The same plot for ¹⁵³Gd.

Time after release at t ₀	MDA _{Gd-148} (Bq)				MDD _{Gd-148} (μSv) Chronic ingestion				MDA _{Gd-148,inh} (Bq) Acute inhalation at t ₀				MDD _{Gd-148,inh} (μSv) Acute inhalation at t ₀			
	1 y op		5 y op		1 y op		5 y op		1 y op		5 y op		1 y op		5 y op	
	115.4 keV	154.6 keV	115.4 keV	154.6 keV	115.4 keV	154.6 keV	115.4 keV	154.6 keV	115.4 keV	154.6 keV	115.4 keV	154.6 keV	115.4 keV	154.6 keV	115.4 keV	154.6 keV
1 d	0.0634	0.121	0.306	0.582	0.0035	0.0067	0.0168	0.032	0.362	0.689	1.74	3.31	4.57	8.68	22.0	41.8
7 d	0.069	0.132	0.334	0.635	0.0178	0.0339	0.0857	0.163	1.68	3.19	8.08	15.4	21.7	40.2	102	194
30 d	0.096	0.183	0.464	0.882	0.107	0.203	0.513	0.975	2.73	5.19	13.18	25.0	34.4	65.4	165	315
1 y	11.6	22.2	56.0	107	168	320	808	1540	481	915	2310	4400	6060	11,500	29,100	55,400

Table 2. Theoretical minimum detectable whole-body activity (MDA) and corresponding minimum detectable committed effective dose (MDD) using either the 115.4 keV or 154 keV photo peaks of ¹⁴⁶Gd as a marker for the whole-body activity of ¹⁴⁸Gd for chronic ingestion and for an acute inhalation for an adult male (AMAD = 2.2 μm).

Detection limits of whole-body burden and cumulative committed effective dose of radiogadolinium isotopes for a high-resolution whole-body counting system. For the 123% HPGe detector setup described by Rääf et al.⁸ with a pulse acquisition time of 2400 s in a Palmer geometry, the estimated minimum detectable activity, MDA, of ¹⁴⁶Gd using the 114 + 115 keV and 154.6 keV gamma lines, and a correction factor for enhanced detectability in the abdominal region by a factor of 2.1 described previously, is estimated to be 6.3 and 12 Bq, respectively, for a homogeneous nuclide distribution in the abdominal region for a 70 kg person. For an activity ratio $a_{146/148}(t)$ of 21.0 (5 years operation tungsten target) at $t=0$, this will give an MDA of 0.31 (using the 115.4 keV peak) and 0.58 Bq (using the 154.6 keV peak) for ¹⁴⁸Gd. The corresponding minimum detectable committed effective dose, $MDD(t) = e_{Gd-148} \cdot t \cdot MDA(t) / q_{Gd-148}(t)$, is 0.017 μSv and 0.032 μSv, respectively, for an acute ingestion just 1 day after the release (Table 2). As the amount of ¹⁴⁸Gd is initially cumulated in the body according to Eq. (3), the detection level will decrease slightly with time; however, within one week, the physical decay of the tracing nuclide ¹⁴⁶Gd will instead lead to an exponentially increasing detection limit. Hence, the corresponding MDA and MDD values (when using the 115.4 keV peak of the ¹⁴⁶Gd isotope) for chronically exposed adults will become 56 Bq and 810 μSv after 1 year post release of a 5 years operated W particle release (Table 2).

If instead ¹⁵³Gd (with either the gamma lines at 97.4 and 103.2 keV, respectively) is used as an indicator of body activity and cumulative committed effective dose of ¹⁴⁸Gd, the detection levels are initially higher than when using ¹⁴⁶Gd due to the relatively lower initial isotope ratio in the released W-target material (e.g., 42.5 vs. 101 for a target under 1 year operation). As mentioned previously, however, 1 year post release it is evident that ¹⁵³Gd will be a much more sensitive indicator for the presence of ¹⁴⁸Gd, with significantly lower MDA and MDD values compared with ¹⁴⁶Gd (Table 3).

For gadolinium in oxide form, up to 50% of inhaled radiogadolinium will be accumulated in the lungs¹²; see also Fig. 7), and the measurement geometry in vivo would therefore be a torso geometry, as previously mentioned in the Section “Estimating ¹⁴⁸Gd whole-body burden and cumulative committed effective dose by means of high-resolution gamma spectrometry”. This gives rise to a corresponding factor of 3.2 increase in MDA of the primary photon peaks in this energy region of ¹⁴⁶Gd and ¹⁵³Gd, compared with assuming an abdominal uptake, and thus a corresponding increase in the indirect determination of ¹⁴⁸Gd. From the results given in Table 2, it

Time after release at t_0	MDA_{Gd-148} (Bq)				MDD_{Gd-148} (μ Sv) Chronic ingestion				$MDA_{Gd-148,inh}$ (Bq) Acute inhalation $t_0 = 0$				$MDD_{Gd-148,inh}$ (μ Sv) Acute inhalation at t_0			
	97.4 keV	103.2 keV	97.4 keV	103.2 keV	97.4 keV	103.2 keV	97.4 keV	103.2 keV	97.4 keV	103.2 keV	97.4 keV	103.2 keV	97.4 keV	103.2 keV	97.4 keV	103.2 keV
1 day	0.443	0.585	1.40	1.85	0.0243	0.0328	0.0767	0.102	2.52	3.33	7.93	10.5	31.8	42.0	100	132
7 day	0.450	0.596	1.42	1.88	0.116	0.153	0.365	0.482	10.9	14.4	34.3	45.4	137	182	432	572
30 day	0.481	0.639	1.52	2.01	0.532	0.704	1.68	2.22	13.6	18.0	42.7	56.6	171	226	539	713
1 year	1.27	1.68	4.01	5.31	18.4	24.3	57.9	76.6	50.9	67.4	160	212	642	849	2020	2670

Table 3. Theoretical minimum detectable whole-body activity (MDA) and corresponding minimum detectable cumulated dose (MDD) using either the 97.4 keV or 103.2 keV photo peaks of ^{153}Gd as a marker for the whole-body activity of ^{148}Gd for chronic ingestion and for an acute inhalation for an adult male (AMAD = 2.2 μm).

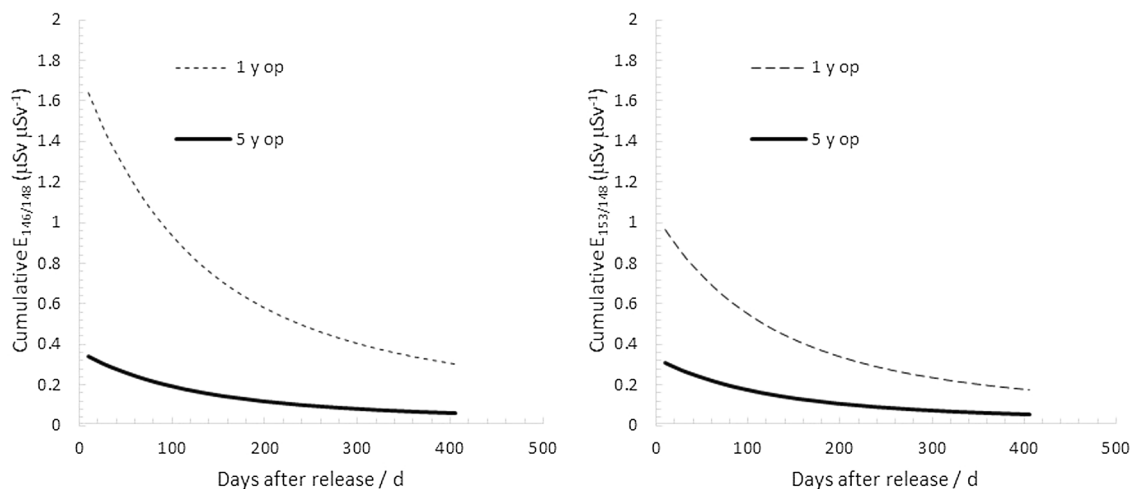


Figure 7. Left: The ratio between the cumulative committed effective dose from ^{146}Gd and ^{148}Gd as a function of time after onset of chronic ingestion of 1 Bq d^{-1} of ^{148}Gd . Right: The same plot for ^{153}Gd .

can be seen that MDD values can be reasonably low ($< 0.20 \text{ mSv}$) using high-resolution whole-body counting of ^{146}Gd as a trace nuclide for the internal dose of ^{148}Gd if measured within 30 days upon release, regardless of whether the uptake occurred through ingestion or inhalation. However, for longer monitoring delays, it appears that ^{153}Gd will be a much more sensitive indicator of inhaled ^{148}Gd , regardless of the operation history of a W target before release. Nevertheless, it will then not be plausible to determine committed effective doses from acute inhalations lower than about 3 mSv , even if using ^{153}Gd (Table 3).

Perturbations in whole-body gamma spectrometry of radiogadolinium. In addition to the theoretical detection limits, the presence of perturbing radionuclides must also be considered. A representative W-target particle was investigated that contained a radionuclide composition according to our calculations². Monte Carlo N-Particle (MCNP) code simulations²⁵ of the emission spectrum from a representative W-target particle are shown in Fig. 8. It appears that a number of perturbing gamma emitters will be present, of which the ^{182}Ta ($t_{1/2} = 114.4 \text{ d}$) peaks at 152.5 keV ($n_g = 0.070$) and 156.4 keV ($n_g = 0.027$) will most definitely affect the 154.6 keV line of ^{146}Gd . Tantalum has uptake properties similar to those of gadolinium (ICRP 119), and inhalation or ingestion of gadolinium may be accompanied with corresponding intakes of ^{182}Ta . Ongoing work will shed light on the time window for in vivo determination of inhaled ^{146}Gd in lungs and of the various potential contributions to the internal dose from spallation source products.

Conclusions

A potential release of W-target material from a spallation source may lead to atmospheric dispersion of radioactive gadolinium which is continuously generated in the target during the spallation operation. According to ICRP, the predominant effective dose contribution of the gadolinium isotopes will be from ^{148}Gd due to its alpha emission and can in an accident scenario with atmospheric dispersion of the nuclides potentially lead to significant internal exposures through inhalation. A theoretical investigation has been done of a method to determine internal exposures from inhaled or ingested ^{148}Gd in affected subjects using in vivo whole-body counting in combination with pre-calculated activity ratios between the alpha emitter ^{148}Gd and the corresponding gamma-emitting gadolinium isotopes ^{146}Gd and ^{153}Gd . ^{146}Gd will initially be the most sensitive indicator of the ^{148}Gd internal dose, but some months after a release event, ^{153}Gd will, in theory, be a much more sensitive ^{148}Gd dose indicator. For a 123% HPGe detector used in Palmer geometry, 1-year post release, in vivo detection of ^{153}Gd

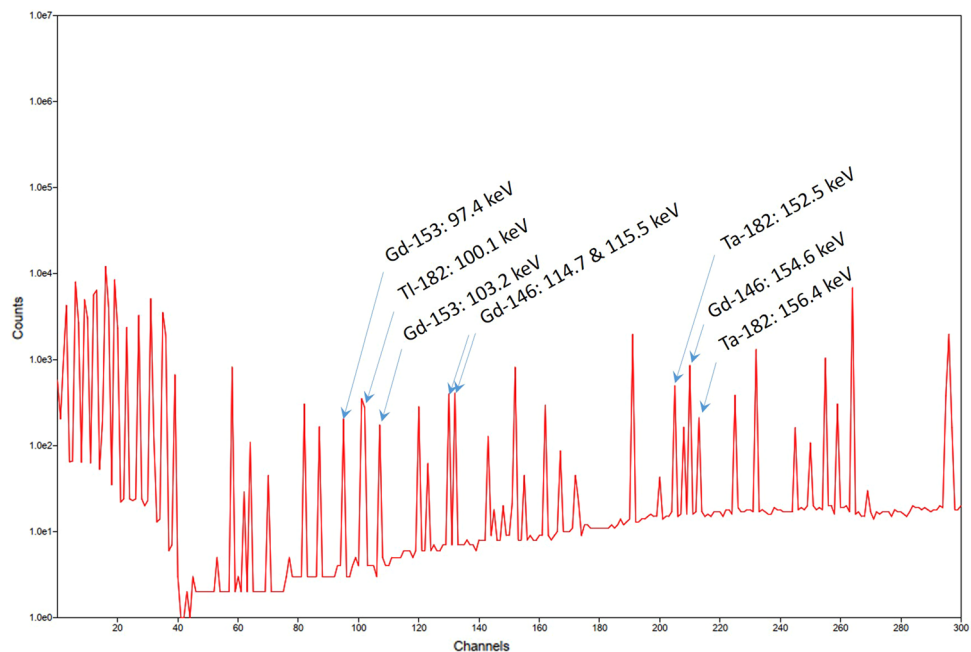


Figure 8. Simulated spectrum from a W spallation target, operated for 5 years. The emission spectrum refers to 50 days post end of operation.

can yield a minimum detectable cumulative committed effective dose from ^{148}Gd ranging from 18 to 77 μSv for ingested ^{148}Gd , and 0.64 to 2.7 mSv for acutely inhaled ^{148}Gd , depending on the operational age of the released spallation target material and on which gamma peak (97.4 or 103.2 keV) is used in the assessment. However, preliminary Monte Carlo simulations of particle emission spectra from a W target in a spallation source being operated for 5 years show that the ^{182}Ta peak may potentially perturb some of the investigated primary gamma lines from ^{146}Gd and ^{153}Gd . If that is the case, in vivo detection of gadolinium uptake can be made indirectly through the ^{146}Gd daughter, ^{146}Eu . This is to be investigated further in continued studies.

Received: 28 July 2020; Accepted: 10 November 2020

Published online: 14 December 2020

References

- Garoby, R. *et al.* The European Spallation Source Design. *Phys. Scr.* **93**(1), 014001 (2018).
- Barkauskas, V. & Stenström, K. Prediction of the radionuclide inventory in the European Spallation Source target using FLUKA. *Nucl. Instrum. Methods Phys. Res., Sect. B* **471**, 24–32 (2020).
- Swedish Radiation Safety Authority (SSM). Underlag till placering i beredskapskategori för ESS och beredskapsplaneringen kring anläggningen. *Report SSM2018–1037–4 (in Swedish)* (2018).
- Lundquist, H. *Radiological Safety Review of the European Spallation Source (ESS)*. Internal report Sweden (ESS) (2013).
- Stankovsky, A., Saito, M., Artisyuk, V., Shmelev, A. & Korovin, Y. Accumulation and transmutation of spallation products in the target of accelerator-driven system. *J. Nuclear Sci. Technol.* **38**(7), 503–510 (2001).
- Malusek, A. & Pettersson, H. *Independent feasibility evaluation of a model for inhalation dose coefficient estimations for exposure of the public* Internal report (Linköping University, Sweden, 2016).
- ICRP. *Compendium of Dose Coefficients based on ICRP Publication 60*. Annals of the ICRP, ICRP Publication 119 (2012).
- Räaf, C., Almén, A., Johansson, L. & Eriksson Stenström, K. In vivo measurement of pre-operational spallation source workers: Baseline body burden levels and detection limits of relevant gamma emitters using high-resolution gamma spectrometry. *J. Radiol. Prot.* **40**(1), 119–133 (2020).
- Firestone, R.B., Ekstrom, L.P., Chu, S.Y.F. WWW Table of Radioactive Isotopes.
- IAEA. *Handbook of parameter values for the prediction of radionuclide transfer in terrestrial and freshwater environments*. IAEA-TRS-472 (2010).
- Lund University, Research grant contract with Swedish Radiation Safety Authority (SSM) *Region-specific radioecological evaluation of releases of radionuclides from ESS – during operation and accidents*. Contract no SSM2019–1010–5, (2019).
- ICRP. *Occupational Intakes of Radionuclides: Part 4*. Annals of the ICRP, ICRP Publication 141 (2019).
- ICRP. *Occupational Intakes of Radionuclides: Part 2*. Annals of the ICRP, ICRP Publication 134 (2016).
- ICRP. *Human Alimentary Tract Model for Radiological Protection*. Annals of the ICRP, ICRP Publication 100 (2006).
- European Spallation Source (ESS). *Tungsten Oxidation and AeroSol Transport (TOAST)*. ESS report ESS-0151001, ESS, Sweden (2018).
- European Spallation Source (ESS). *Description of the bounding target loss of cooling accident*. ESS report ESS-0092293, ESS, Sweden (2018).
- CERN. *FLUKA: A Multi-Particle Transport Code*. CERN report CERN–2005–010 (2005).
- Böhlen, T. T. *et al.* The FLUKA Code: Developments and Challenges for High Energy and Medical Applications. *Nucl. Data Sheets* **120**, 211–214 (2014).
- Shutt, A. L. *et al.* A study of the human biokinetics of inhaled gadolinium oxide. *Ann. Occup. Hyg.* **46**(Suppl_1), 320–322 (2002).
- IMBA. Integrated Modules for Bioassay Analysis. Internal Dosimetry Software. Public Health England (PHE), UK (2020).

21. Kókai, Z. *et al.* Comparison of different target material options for the European Spallation Source based on certain aspects related to the final disposal. *Nucl. Instrum. Methods Phys. Res., Sect. B* **416**, 1–8 (2018).
22. European Spallation Source (ESS). *Preliminary Safety Analysis Report*. ESS, Sweden (2012).
23. Visual Monte Carlo (VMC). Software for radiation protection and internal dosimetry. Available from: <http://vmcsoftware.com/Index.html> (2018). Accessed 3 November 2020.
24. ICRP. *Occupational Intakes of Radionuclides: Part 1*. Annals of the ICRP, ICRP Publication 130 (2015).
25. Werner, C.J., *et al.*, *MCNP Version 6.2 Release Notes*. Los Alamos National Laboratory report LA-UR-18–20808, United States (2018).

Acknowledgements

This project has been funded by the Swedish Radiation Safety Authority (SSM 2007_2984_32, SSM2018-1636 and SSM2016-1586).

Author contributions

C.L.R. conceived and designed the work, contributed to the data collection and graphical presentation, performed the data analysis and interpretation, the drafting of the article and the final approval of the submitted version. V.B. conceived the work and contributed to the main data collection and graphical presentation. K.S.E. critically reviewed the article and contributed to the literature survey. C.B. critically reviewed the article and contributed to the literature survey. H.P. contributed to the data collection and graphical presentation, contributed to the literature survey and to the critical revision of the article.

Funding

Open Access funding provided by Lund University.

Competing interests

The authors declare no competing interests.

Additional information

Correspondence and requests for materials should be addressed to C.R.

Reprints and permissions information is available at www.nature.com/reprints.

Publisher's note Springer Nature remains neutral with regard to jurisdictional claims in published maps and institutional affiliations.



Open Access This article is licensed under a Creative Commons Attribution 4.0 International License, which permits use, sharing, adaptation, distribution and reproduction in any medium or format, as long as you give appropriate credit to the original author(s) and the source, provide a link to the Creative Commons licence, and indicate if changes were made. The images or other third party material in this article are included in the article's Creative Commons licence, unless indicated otherwise in a credit line to the material. If material is not included in the article's Creative Commons licence and your intended use is not permitted by statutory regulation or exceeds the permitted use, you will need to obtain permission directly from the copyright holder. To view a copy of this licence, visit <http://creativecommons.org/licenses/by/4.0/>.

© The Author(s) 2020